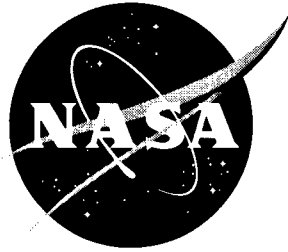# Simulation of Fatigue Crack Initiation at Corrosion Pits With EDM Notches

Stephen W. Smith
Langley Research Center, Hampton, Virginia

John A. Newman
U.S. Army Research Laboratory
Vehicle Technology Directorate
Langley Research Center, Hampton, Virginia

Robert S. Piascik
Langley Research Center, Hampton, Virginia

March 2003

The NASA STI Program Office ... in Profile

Since its founding, NASA has been dedicated to the advancement of aeronautics and space science. The NASA Scientific and Technical Information (STI) Program Office plays a key part in helping NASA maintain this important role.

The NASA STI Program Office is operated by Langley Research Center, the lead center for NASA's scientific and technical information. The NASA STI Program Office provides access to the NASA STI Database, the largest collection of aeronautical and space science STI in the world. The Program Office is also NASA's institutional mechanism for disseminating the results of its research and development activities. These results are published by NASA in the NASA STI Report Series, which includes the following report types:

- TECHNICAL PUBLICATION. Reports of completed research or a major significant phase of research that present the results of NASA programs and include extensive data or theoretical analysis. Includes compilations of significant scientific and technical data and information deemed to be of continuing reference value. NASA counterpart of peer-reviewed formal professional papers, but having less stringent limitations on manuscript length and extent of graphic presentations.

- TECHNICAL MEMORANDUM. Scientific and technical findings that are preliminary or of specialized interest, e.g., quick release reports, working papers, and bibliographies that contain minimal annotation. Does not contain extensive analysis.

- CONTRACTOR REPORT. Scientific and technical findings by NASA-sponsored contractors and grantees.

- CONFERENCE PUBLICATION. Collected papers from scientific and technical conferences, symposia, seminars, or other meetings sponsored or co-sponsored by NASA.

- SPECIAL PUBLICATION. Scientific, technical, or historical information from NASA programs, projects, and missions, often concerned with subjects having substantial public interest.

- TECHNICAL TRANSLATION. English-language translations of foreign scientific and technical material pertinent to NASA's mission.

Specialized services that complement the STI Program Office's diverse offerings include creating custom thesauri, building customized databases, organizing and publishing research results ... even providing videos.

For more information about the NASA STI Program Office, see the following:

- Access the NASA STI Program Home Page at *http://www.sti.nasa.gov*

- E-mail your question via the Internet to help@sti.nasa.gov

- Fax your question to the NASA STI Help Desk at (301) 621-0134

- Phone the NASA STI Help Desk at (301) 621-0390

- Write to:
  NASA STI Help Desk
  NASA Center for AeroSpace Information
  7121 Standard Drive
  Hanover, MD 21076-1320

Simulation of Fatigue Crack Initiation at Corrosion Pits With EDM Notches

Stephen W. Smith
Langley Research Center, Hampton, Virginia

John A. Newman
U.S. Army Research Laboratory
Vehicle Technology Directorate
Langley Research Center, Hampton, Virginia

Robert S. Piascik
Langley Research Center, Hampton, Virginia

March 2003

Abstract

Uniaxial fatigue tests were conducted to compare the fatigue life of laboratory produced corrosion pits, similar to those observed in the shuttle main landing gear wheel bolt-hole, and an electro-discharged-machined (EDM) flaw. EDM flaws are used to simulate corrosion pits during shuttle wheel (dynamometer) testing. The aluminum alloy (AA 7050) laboratory fatigue tests were conducted to simulate the local stress level contained in the wheel bolt-hole. Under this high local stress condition, the EDM notch produced a fatigue life similar to test specimens containing corrosion pits of similar size. Based on the laboratory fatigue test results, the EDM flaw (semi-circular disc shaped) produces a local stress state similar to corrosion pits and can be used to simulate a corrosion pit during the shuttle wheel dynamometer tests.

Introduction

During a scheduled maintenance inspection of an orbiter (shuttle vehicle), visual inspection of forged aluminum alloy (AA 7050) main landing gear (MLG) wheels revealed small regions of localized corrosion (pitting) in the tie-bolt holes shown in Figure 1. The photograph in Figure 2 shows a typical tie-bolt hole containing corrosion pits. Inspections revealed that most pits were less than 0.5 mm (0.02 inch) deep, but a few pits were as deep as 1.0 mm (0.04 inch). A common procedure in the aerospace industry is to remove corrosion pitting by grinding. However, if any corrosion damage is still present after assembly, increased local stress at the pits may result in reduced fatigue strength of the component [1], *i.e.*, fatigue cracking may occur during shuttle roll out, landing, *etc*.

To determine the effect of pitting on shuttle wheel fatigue life, a series of shuttle wheel dynamometer fatigue tests were planned. However, there were no MLG wheels available for testing containing corrosion pits consistent with the "worst case" in-service damage. Therefore, it was necessary to produce such a flaw in each MLG wheel article prior to testing. For aluminum alloys, corrosion pit configuration is associated with local microstructure (constituent particles, precipitates, and grain boundaries). Consequently, the location of corrosion pits is difficult to control and a wide range of pit morphologies can result when components are corroded, even in a laboratory environment. Additionally, it is difficult to control the location of individual pits. Therefore, the generation of corrosion pits on MLG wheels may result in the formation of pits that are not consistent with those produced in-service; thereby, resulting in tests

that do not replicate service conditions. Because manufactured defects (electro-discharge machined (EDM) notches) can be fabricated more consistently than corrosion pits and there are limited MLG wheels available for testing, EDM notches were machined in MLG wheels to simulate the local stress states produced by corrosion pits. However, this approach raises the question of whether the fatigue behavior of MLG wheels containing EDM notches is similar to that of in-service components. The present investigation was undertaken to answer this question.

The configuration of each corrosion pit affects the initiation and nucleation of fatigue cracks [1]. This work was performed to determine if an EDM notch will result in a similar reduction in fatigue strength of an AA7050 component containing corrosion pits similar to those observed in the MLG wheels (See Figure 3). Mechanical test specimens containing either an EDM notch or a corrosion pit were examined under fatigue loading at stress levels representative of the service loading in the bolt-hole region and the fatigue life of each specimen was determined.

Test Procedure

The shuttle MLG wheel is forged and constructed of aluminum alloy AA 7050. Because the forged wheel configuration is complex, it is extremely difficult to simulate the exact microstructural attributes (*e.g.*, constituent particles, precipitates, and grain boundaries) that produce corrosion pits of the size, shape and morphology similar to corrosion pits observed in the fastener hole region. Therefore, axially loaded fatigue specimens were machined from AA7050 plate in two different orientations. (See Figure 4.) Both specimen configurations were produced with the loading axis parallel to the rolling direction and with a nominal gage section that was 25.4 mm (1.0 inch) wide and 12.7 mm (0.5 inch) thick. The defect (either an EDM notch or corrosion pit) was located in the center of the gage section on a 25.4 mm wide surface as indicated by the hatched region shown in Figure 4 (one side only). For L-S orientation specimens (loading axis parallel to the longitudinal direction and the major crack growth direction parallel to the short-transverse direction), defects were produced on a surface of the specimen parallel to the longitudinal and long-transverse directions. For L-T orientation specimens (loading axis parallel to the longitudinal direction and the major crack growth direction parallel to the long-transverse direction), defects were produced on a surface of the

specimen parallel to the longitudinal and short-transverse directions. Because of the grain structure in a rolled plate, corrosion pits produced in L-S and L-T specimen orientations result in a wide range of configurations and morphologies. The L-S specimen orientation exposes fewer grain boundaries leading to broad shallow pits that are nearly hemispherical in shape (lower local stress concentration factor, k_t). The L-T specimen orientation, on the other hand, exposes more grain boundaries, constituent stringers, etc., leading to more irregular shaped and possibly elongated pits (higher local k_t). The EDM notches used to simulate a corrosion pit stress concentration were semicircular with a height of approximately 0.254 mm (0.01 inch), a depth (a) and surface width ($2c$). (See Figure 5.) The depth and width of each EDM notch and corrosion pit is summarized in Tables 1 and 2.

To produce corrosion pits, specimens were coated with a protective wax and a small · "pinhole" in the wax was introduced to expose a small region in the center of the specimen gage section (hatched region in Figure 4). The specimens were then immersed in an aqueous solution containing 3-g/L sodium chloride (NaCl) and 0.11 N nitric acid (HNO_3). A graphite counter electrode was also placed into the solution and electrically coupled to the test specimens and potentiostat. Three specimens were coupled together and corroded simultaneously by applying an anodic current of 1.0 mA for the L-S specimens and 2.5 mA for the L-T specimens. A larger current was applied to the L-T specimens to compensate for a lower corrosion rate observed for the L-T orientation compared to the L-S orientation. To produce a variety of pit sizes in the desired range sizes, 0.5 mm (0.02 inch) $< a <$ 1.5 mm (0.06 inch), total exposure times were varied from 24 to 96 hours.

Following the introduction of surface defects (EDM notch or corrosion pit), specimens were fatigue tested using a closed-loop servo-hydraulic test machine. Specimens were cyclically loaded (constant amplitude) at a maximum load of P_{max} = 100 kN (22,500 lbs) and a load ratio, R = 0.05 (P_{min} = 5 kN or 1,125 lbs). A maximum remote stress of σ_{max} = 310 MPa (45 ksi), approximately 70% of the yield stress (σ_y = 452 MPa [2]), was used to simulate the service stress in the shuttle MLG wheel bolt-hole region.[1] Testing was performed in room-temperature laboratory air at a loading frequency of 4 Hz. Periodically, fatigue loading was stopped for approximately 1 minute (specimen was held at mean load, P_{mean} = 52.5 kN (11.81 kips)) while visual surface crack length, $2c$, measurements were made. Fatigue loading continued until

---

[1] NASA - Johnson Space Flight Center (JSC) specified the maximum remote stress level.

specimen failure occurred, *i.e.*, the specimen fractured into two pieces. The fractured surfaces of each specimen were examined using a scanning electron microscope (SEM) and the EDM notch or corrosion pit dimensions were measured.

Results and Discussion

Surface crack-length versus load cycle ($2c$ versus N) data is plotted in Figures 6a and 6b for L-S and L-T specimens, respectively. All fatigue cracks exhibited similar fatigue crack growth rate ($d2c/dN$) characteristics. The fatigue test results shown in Figure 6 indicate a large variation in the number of load cycles required to produce a detectable fatigue crack. The number of cycles to initiate a visually detectable surface fatigue crack, N_i, and the number of cycles at specimen failure, N_f, are listed in Tables 1 and 2. In all cases, specimen failure was caused by fatigue cracks that initiated from the gage-section flaw (corrosion pit or EDM notch) and propagated by sub-critical fatigue crack growth (typical crack length at fracture was 19 mm (0.75 inches)) followed by final facture. The crack surfaces and typical EDM flaw configurations for two L-S oriented specimens are shown Figure 7. The EDM flaw configuration shown here is also representative of those in specimens of the L-T orientation. Some EDM notches exhibited small irregularities; typical irregularities are noted (arrows) in Figure 7. These small irregularities had no detectable effect on fatigue crack shape or growth rate.

The SEM micrographs shown in Figures 8 and 9 reveal the corrosion pit morphology and the region of fatigue crack initiation for specimens in the L-S and L-T orientations, respectively. The micrographs were used to estimate the corrosion pit shape (dashed lines) characterized by values of a_i and $2c_i$ listed in Tables 1 and 2. The corrosion pits in the L-S specimens (Figure 8) were nearly hemispherical in shape. The region of fatigue crack nucleation in the L-T specimens shown in Figures 9a, c and d contained multiple pits. The dashed line estimates an "affected pit region", which is characterized by a_i and $2c_i$ as listed in Table 2. In Figures 9b and e, dashed lines outline a single pit; the single pit was likely formed when multiple smaller pits (similar to those in Figures 9a, c and d) coalesced. The pits shown in Figures 9b and e exhibit a greater aspect ratio (depth/width ratio) than pits in the L-S specimen orientation (Figure 8). The configuration of the pits in the L-T orientation is a result of greater grain boundary exposure for

4

pitting compared to that found in the L-S specimens. For both the L-S and L-T orientations, it is likely that multiple small fatigue cracks nucleated along the irregular pit surface. The small fatigue cracks rapidly coalesced into a single crack having a stable (nearly semi-circular in shape) crack front configuration. The single surface fatigue crack continued to propagate until unstable crack growth was followed by fracture. Figure 10 is a metallographic cross-section of the pit shown in Figure 8b. Here, the fracture surface was removed by polishing; the micrograph shows a cross-section of the corrosion pit and its morphology on the plane slightly below but very near the fatigue crack surface. The root of this L-S specimen pit exhibits an irregular surface and local intergranular attack (See Figure 10b.) similar that observed in the MLG wheel pits (Compare with Figure 3.).

Plots of initial flaw depth (a_i) versus the cycles to failure (N_f) for L-S and L-T orientation specimens are displayed in Figures 11 and 12, respectively. These data show that specimens containing EDM notches exhibit comparable fatigue behavior to specimens containing corrosion pits. Here, a similar increase in fatigue life is observed with decreasing EDM (closed symbols) and pit (open symbols) flaw depth. Figure 13 reveals that the fatigue properties for L-S and L-T orientation specimens containing EDM and pit flaws are similar. These results show that at a high local stress level fatigue behavior is largely insensitive to significant differences in flaw morphology. At the maximum remote stress of $\sigma_{max} = 310$ MPa (45 ksi), the local stress at the surface flaw results in yielding at the root of the flaw. Thus, crack nucleation is so rapid at this high stress level that geometric differences between EDM flaws and corrosion pits are a second order effect.

Concluding Remarks

Test results showed that corrosion pits, with a variety of configurations and morphologies, and EDM notches produce similar fatigue behavior in both L-S and L-T orientation specimens of AA 7050. As a result of high local stress levels and local yielding, fatigue cracks rapidly nucleated at both EDM flaws and corrosion pits, leading to similar fatigue lives. Because crack nucleation is rapid at high local stress levels, flaw geometry and other

effects are likely to become second order.[2] At lower local stress levels, these effects may become first order and alter the fatigue life. Based on the results of laboratory fatigue tests conducted at a high stress level, representative of service loading in the bolt-hole region of MLG wheels, EDM notches produce a local stress state similar to that for corrosion pits. Thus, EDM notches can be used to simulate the effect of corrosion pits during the shuttle wheel dynamometer tests.

References

1. G.H. Bray, R.J. Bucci, E.L. Colvin, and M. Kulak. "Effects of Prior Corrosion on the S/N Fatigue Performance of Aluminum Sheet Alloys 2024-T3 and 2524-T3", Effects of the Environment on the Initiation of Crack Growth, ASTM STP 1298, W.A. Van Der Sluys, R.S. Piascik, and R. Zawierucha, Eds., ASTM, 1997, pp. 89-103.

2. J. R. Davis, Editor. *Aluminum and Aluminum Alloys*, ASM International, Materials Park, OH, 1993, pp. 694-697.

---

[2] Other effects may include local embrittlement caused by corrosion, local high k_t produced by highly irregular corroded surfaces within the corrosion pit, etc. These effects become less important when the pit or EDM flaw is dominated by plasticity and crack nucleation and small crack growth rates becomes extremely rapid.

Table 1. Summary of flaw characteristics and fatigue data for L-S specimens.

specimen	flaw type	a_i (mm)	$2c_i$ (mm)	N_f	N_i
LS-N-1	EDM notch	1.02	2.37	10,327	1,848
LS-N-2	EDM notch	0.84	2.32	11,349	2,011
LS-N-3	EDM notch	0.89	2.32	10,502	3,509
LS-N-4	EDM notch	0.52	1.43	16,946	5,014
LS-N-5	EDM notch	0.68	1.49	13,835	3,390
LS-N-6	EDM notch	1.47	3.17	7,881	1,005
LS-P-1	Corrosion pit	0.85	2.63	19,698	10,010
LS-P-2	Corrosion pit	1.24	2.39	10,852	3,504
LS-P-3	Corrosion pit	0.68	2.64	18,761	6,206
LS-P-4	Corrosion pit	0.29	1.29	30,472	20,009
LS-P-5	Corrosion pit	0.91	2.59	10,383	2,009

Table 2. Summary of flaw characteristics and fatigue data for L-T specimens.

| specimen	flaw type	a_i (mm)	$2c_i$ (mm)	N_f	N_i
LT-N-1	EDM notch	0.51	1.15	17,627	6,005
LT-N-2	EDM notch	0.79	1.72	12,853	4,523
LT-N-3	EDM notch	0.83	1.71	12,343	2,513
LT-N-4	EDM notch	0.96	1.95	12,021	2,516
LT-N-5	EDM notch	1.09	2.31	11,366	3,513
LT-N-6	EDM notch	1.31	2.87	9,352	2,011
LT-N-7	EDM notch	1.59	3.40	7,192	1,524
LT-P-1	Corrosion pit	0.51	1.14	30,861	24,024
LT-P-2	Corrosion pit	0.49	0.76	16,425	5,002
LT-P-3	Corrosion pit	0.21	1.27	32,490	19,024
LT-P-4	Corrosion pit	0.44	1.62	24,282	18,017
LT-P-5	Corrosion pit	1.51	2.29	10,984	7,812
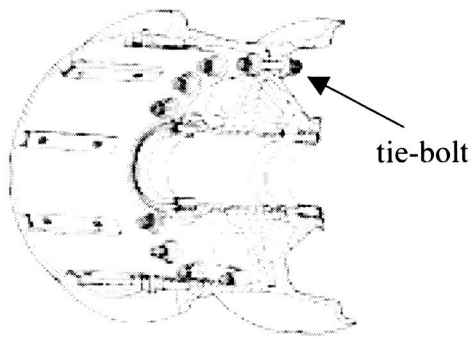
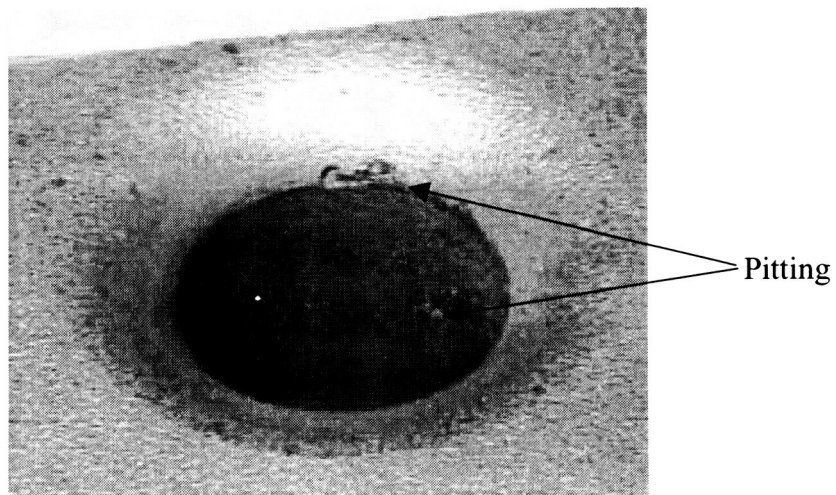Figure 1. Schematic of MLG wheel outer half.

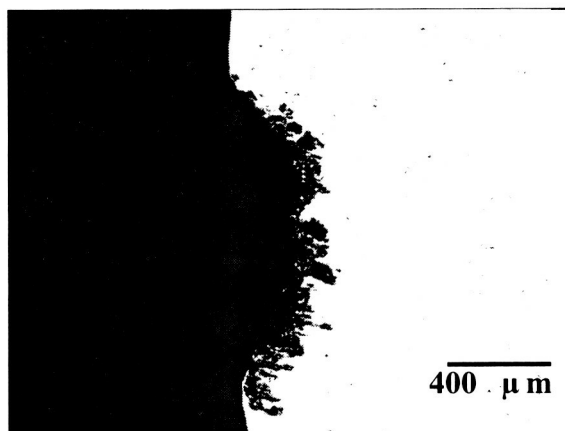Figure 2. Typical MLG wheel tie-bolt pitting.

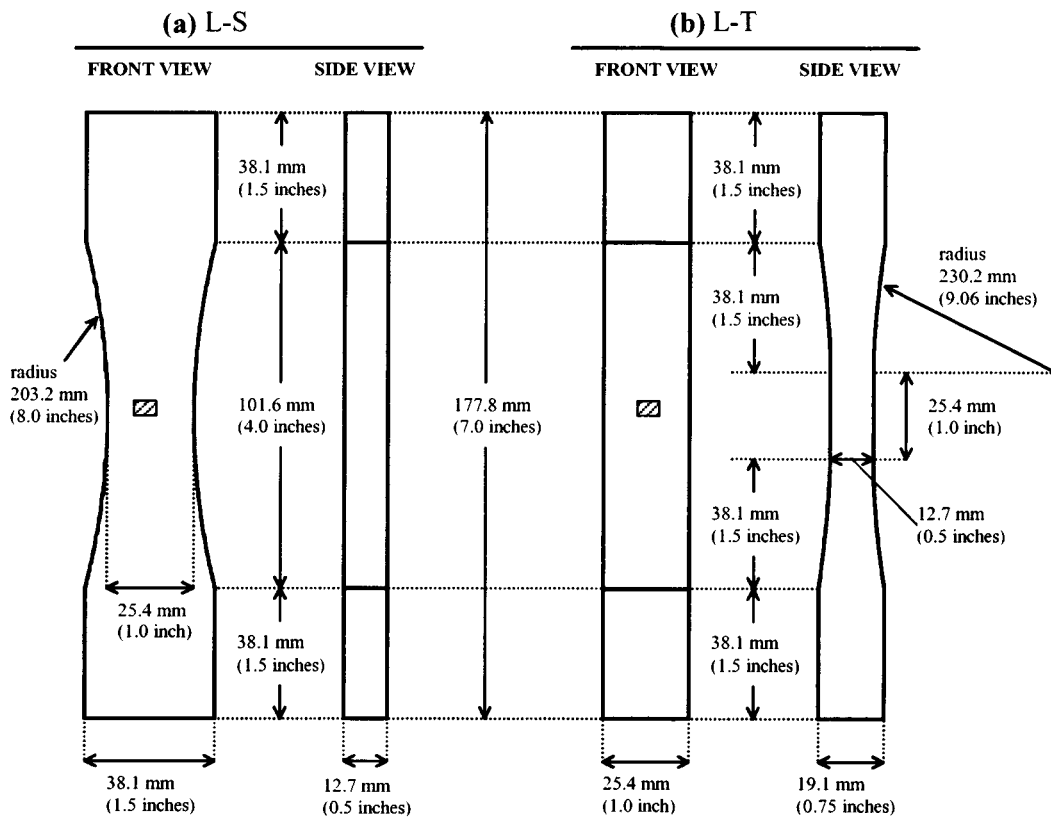Figure 3. Metallographic cross-section of a MLG wheel tie-bolt hole pit.

Figure 4. Fatigue specimen configurations for: (a) L-S specimen, (b) L-T specimen. The hatched region in the center of the gage section represents the location of the corrosion pit or EDM notch.
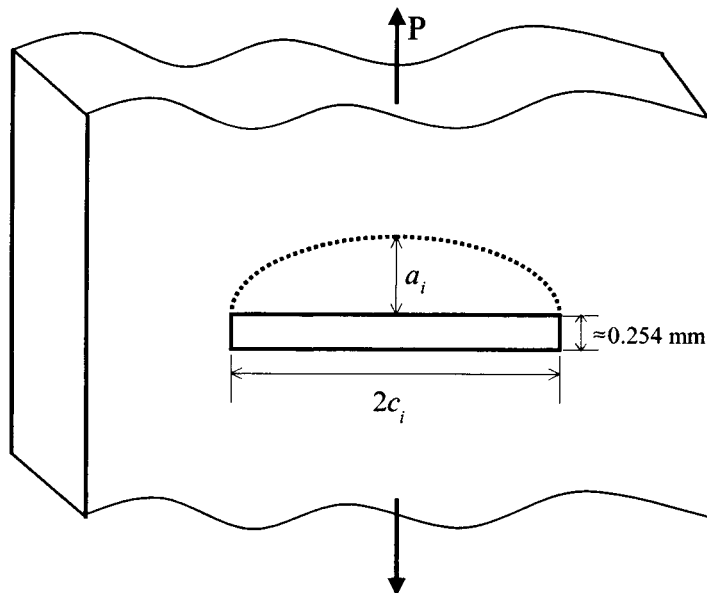

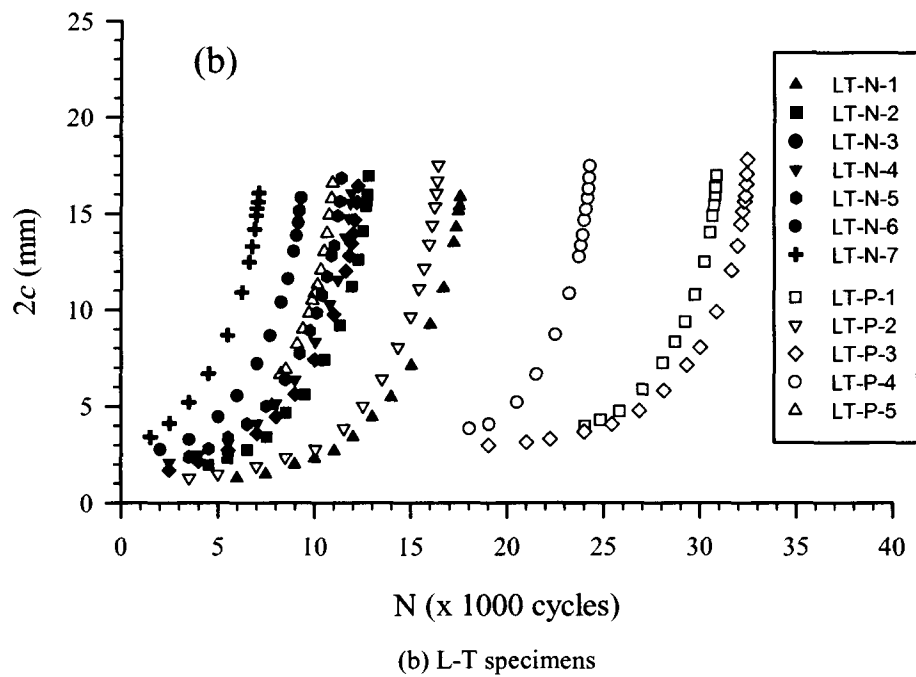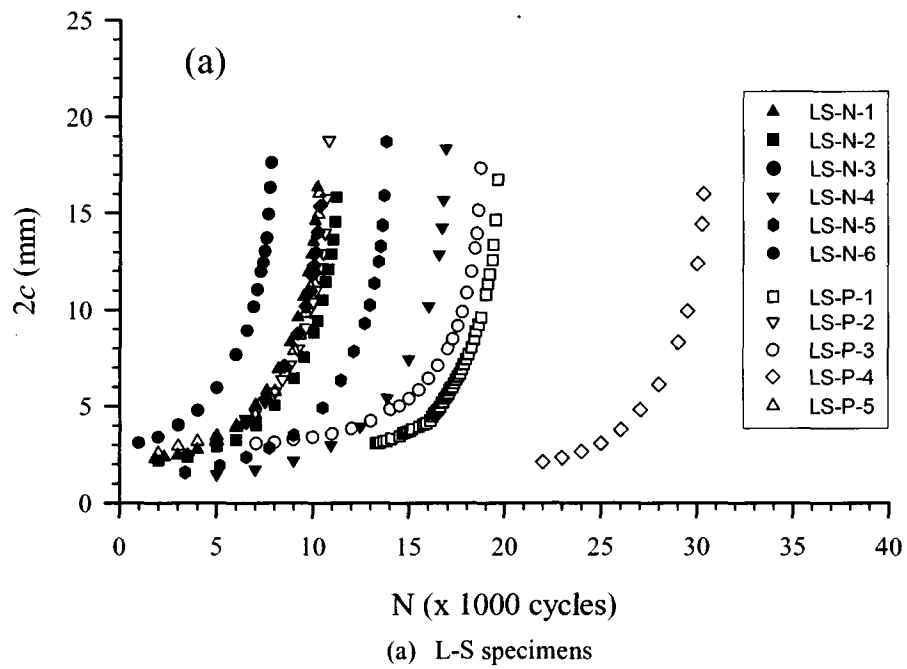
Figure 5. A schematic of the EDM notch configuration.

Figure 6. Surface crack length (2c) versus load cycle count (N) data plotted for AA 7050 (a) L-S specimens and (b) L-T specimens. Open and solid symbols are used for pitted and EDM notch specimens, respectively.
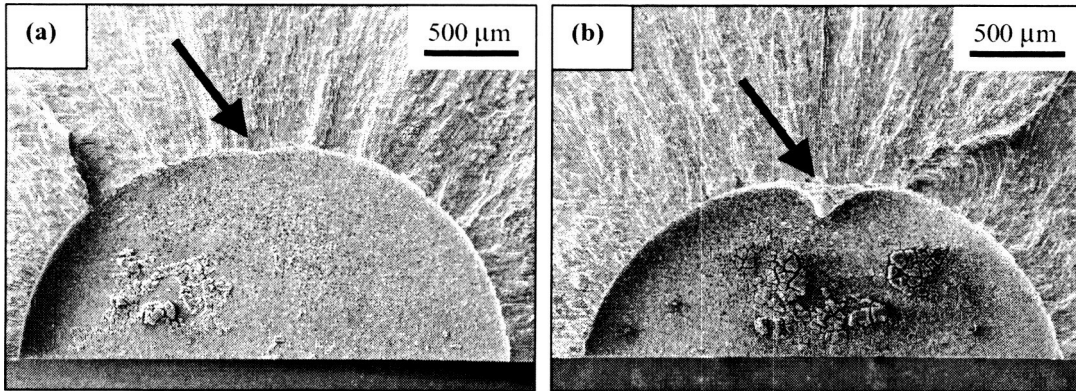
Figure 7. Typical fracture-surface SEM micrographs of EDM notched AA 7050 specimens in the L-S orientation: (a) LS-N-1 and (b) LS-N-2. Small irregularities were observed for some of the EDM notches, as indicated by arrows in the figures.
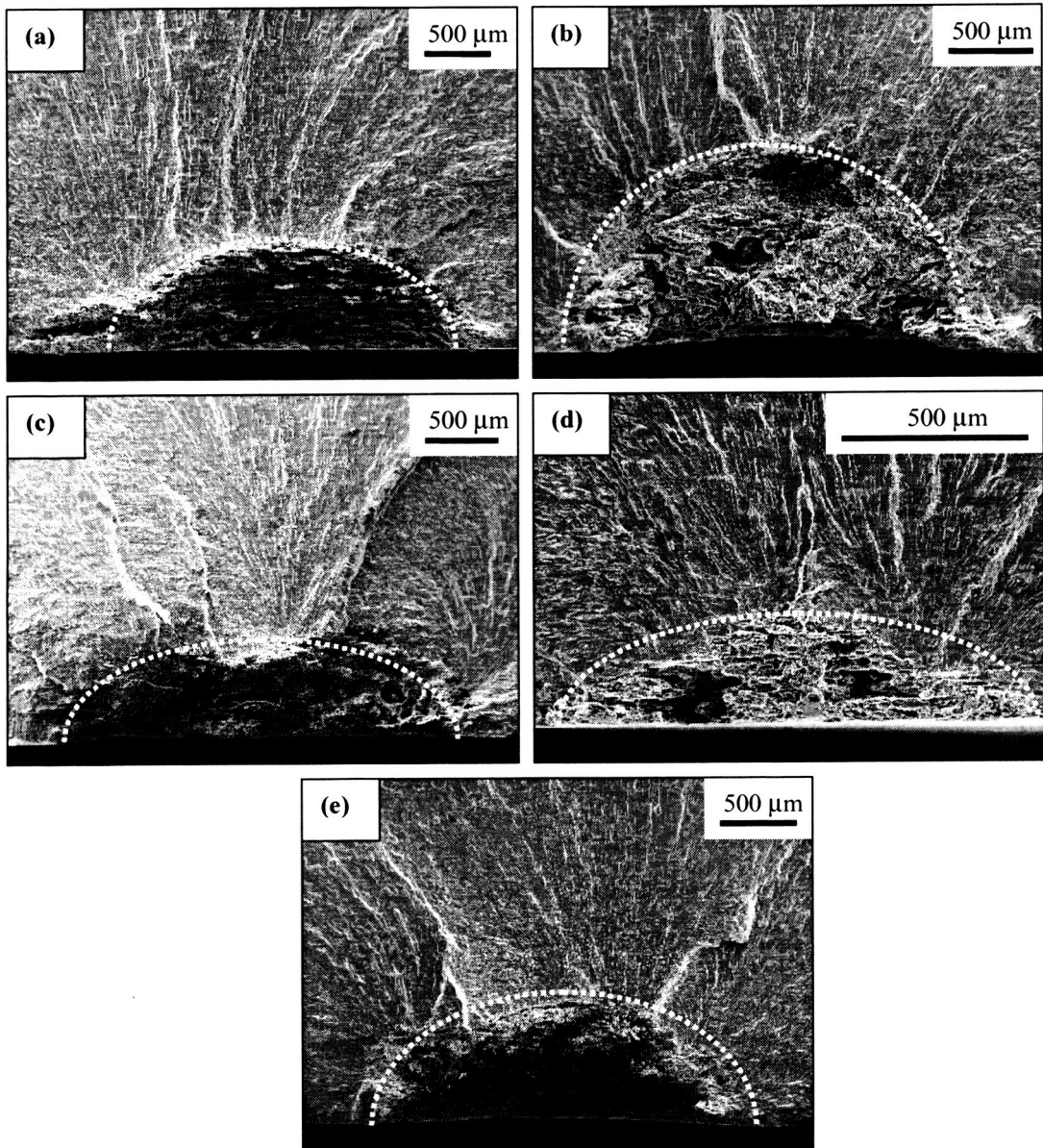
Figure 8. Fracture-surface SEM micrographs of corrosion pitted AA 7050 specimens in the L-S orientation (a) LS-P-1, (b) LS-P-2, (c) LS-P-3, (d) LS-P-4 and (e) LS-P-5.
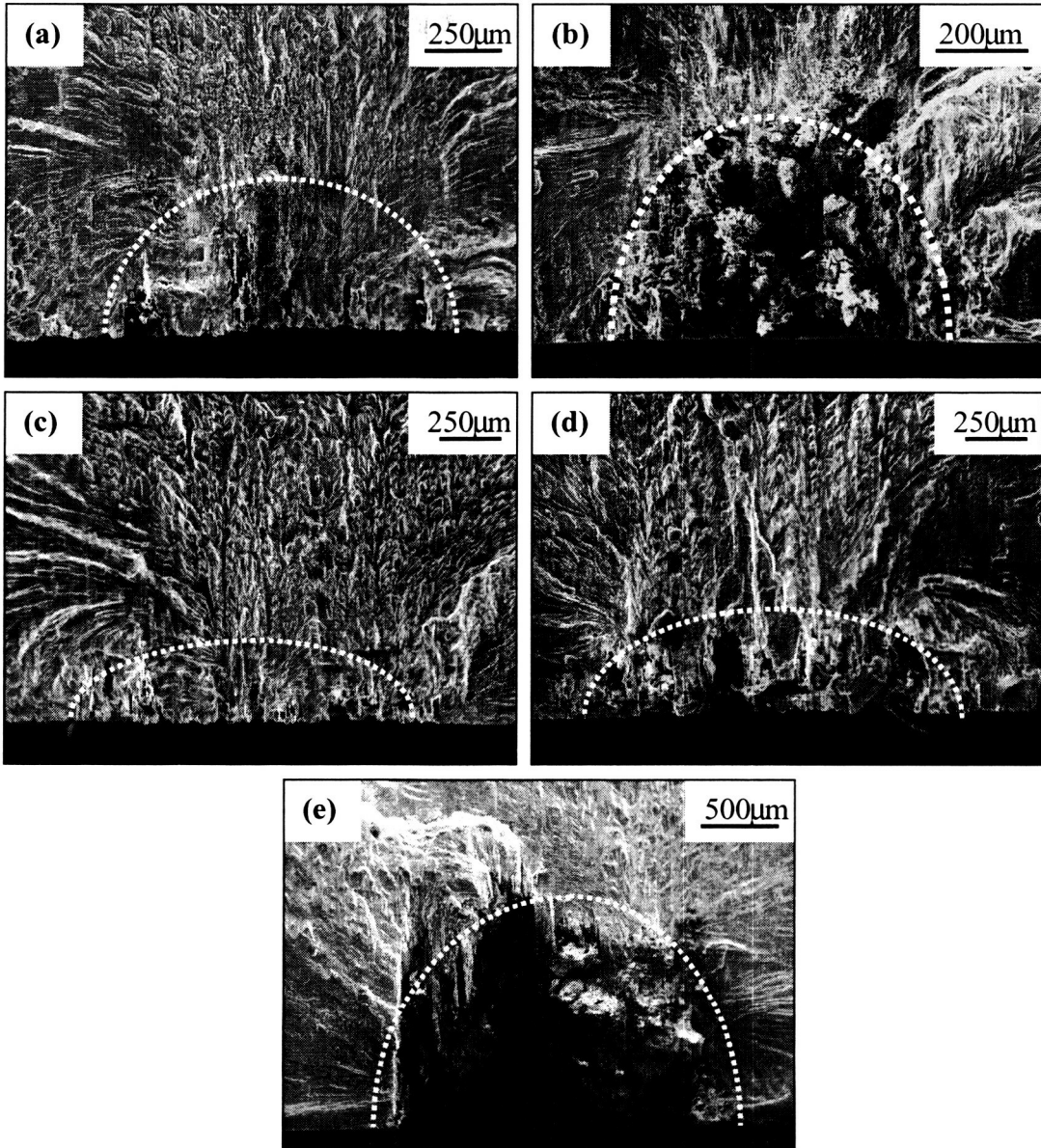
Figure 9. Fracture-surface SEM micrographs of corrosion pitted AA 7050 specimens in the L-T orientation (a) LT-P-1, (b) LT-P-2, (c) LT-P-3, (d) LT-P-4 and (e) LT-P-5.
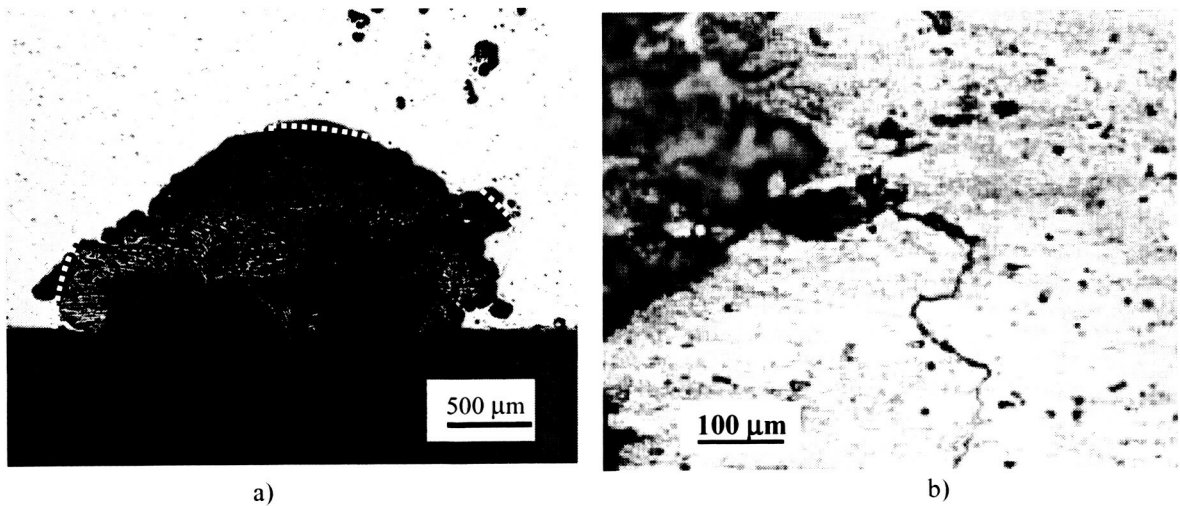
a)

b)

Figure 10. (a) Fracture surface of AA 7050 specimen LS-P-2 in the L-S orientation, polished to reveal corrosion pit configuration. (b) Higher magnification view of the root of the pit after the surface has been lightly etched to reveal evidence of intergranular cracking.
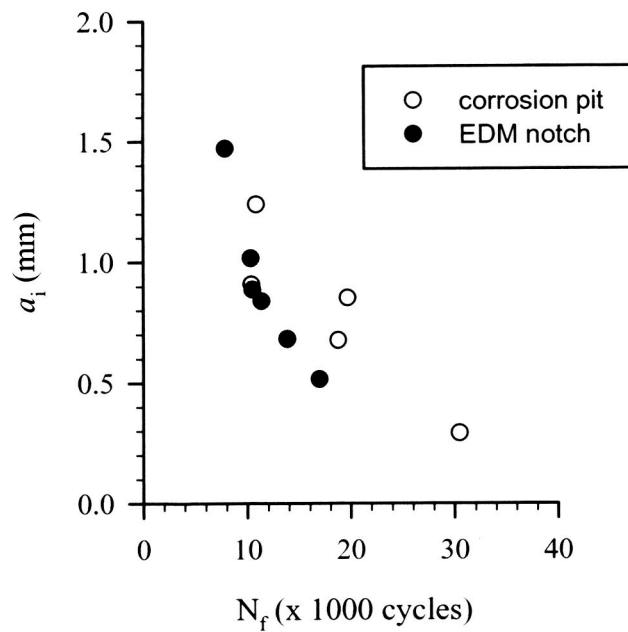

Figure 11. Fatigue life data plotted as flaw depth, a_i, versus cycles to failure, N_f, for AA 7050 specimens in the L-S orientation. Open and solid symbols are used for corrosion-pit and EDM notch specimens, respectively.
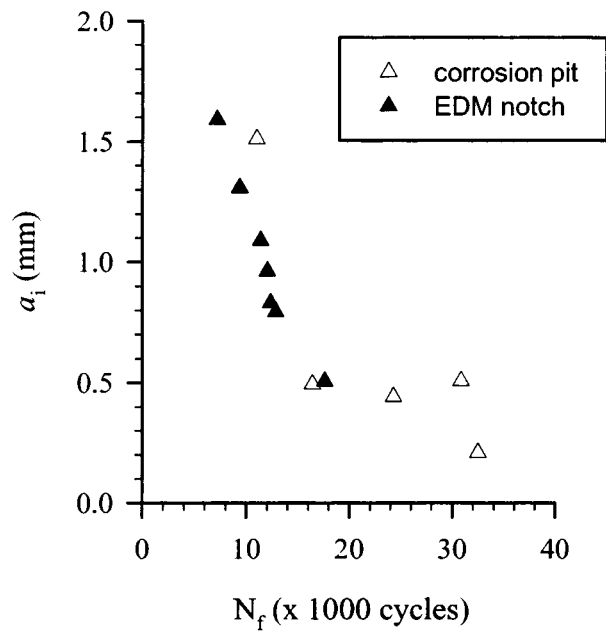
Figure 12. Fatigue life data plotted as flaw depth, a_i, versus cycles to failure, N_f, for AA 7050 specimens in the L-T orientation. Open and solid symbols are used for corrosion-pit and EDM notch specimens, respectively.

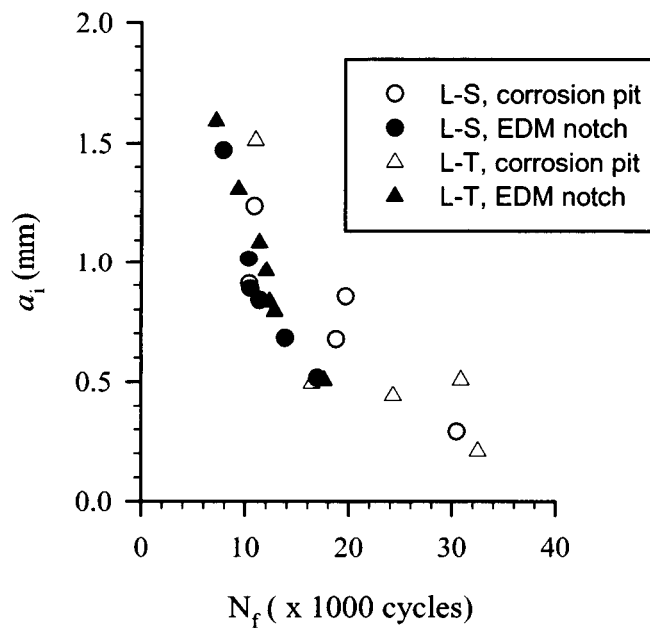

Figure 13. Fatigue life data plotted as flaw depth, a_i, versus cycles to failure, N_f, for AA 7050 specimens in the L-S and L-T orientations. Open and solid symbols are used for corrosion-pit and EDM notch specimens, respectively.

15

REPORT DOCUMENTATION PAGE

Public reporting burden for this collection of information is estimated to average 1 hour per response, including the time for reviewing instructions, searching existing data sources, gathering and maintaining the data needed, and completing and reviewing the collection of information. Send comments regarding this burden estimate or any other aspect of this collection of information, including suggestions for reducing this burden, to Washington Headquarters Services, Directorate for Information Operations and Reports, 1215 Jefferson Davis Highway, Suite 1204, Arlington, VA 22202-4302, and to the Office of Management and Budget, Paperwork Reduction Project (0704-0188), Washington, DC 20503.

1. AGENCY USE ONLY (Leave blank)	2. REPORT DATE	3. REPORT TYPE AND DATES COVERED
	March 2003	Technical Memorandum

4. TITLE AND SUBTITLE
Simulation of Fatigue Crack Initiation at Corrosion Pits With EDM Notches

5. FUNDING NUMBERS
762-60-61-09

6. AUTHOR(S)
Stephen W. Smith, John A. Newman, and Robert S. Piascik

7. PERFORMING ORGANIZATION NAME(S) AND ADDRESS(ES)

NASA Langley Research Center
Hampton, VA 23681-2199

U.S. Army Research Laboratory
Vehicle Technology Directorate
NASA Langley Research Center
Hampton, VA 23681-2199

8. PERFORMING ORGANIZATION REPORT NUMBER

L-18262

9. SPONSORING/MONITORING AGENCY NAME(S) AND ADDRESS(ES)

National Aeronautics and Space Administration
Washington, DC 20546-0001
and
U.S. Army Research Laboratory
Adelphi, MD 20783-1145

10. SPONSORING/MONITORING AGENCY REPORT NUMBER

NASA/TM-2003-212166
ARL-TR-2927

11. SUPPLEMENTARY NOTES

12a. DISTRIBUTION/AVAILABILITY STATEMENT

Unclassified-Unlimited
Subject Category 26   Distribution: Nonstandard
Availability: NASA CASI (301) 621-0390

12b. DISTRIBUTION CODE

13. ABSTRACT (Maximum 200 words)

Uniaxial fatigue tests were conducted to compare the fatigue life of laboratory produced corrosion pits, similar to those observed in the shuttle main landing gear wheel bolt-hole, and an electro-discharged-machined (EDM) flaw. EDM flaws are used to simulate a corrosion pit during shuttle wheel (dynamometer) testing. The aluminum alloy (AA 7050) laboratory fatigue tests were conducted to simulate the local stress level contained in the wheel bolt-hole. Under this high local stress condition, the EDM notch produced a fatigue life similar to test specimens containing corrosion pits. Based on the laboratory fatigue test results, the EDM flaw (semi-circular disc shaped) produces a local stress state similar to corrosion pits and can be used to simulate a corrosion pit during the shuttle wheel dynamometer tests.

14. SUBJECT TERMS
Corrosion pit, EDM notch, fatigue crack initiation, aluminum alloy 7050

15. NUMBER OF PAGES
20

16. PRICE CODE

17. SECURITY CLASSIFICATION OF REPORT	18. SECURITY CLASSIFICATION OF THIS PAGE	19. SECURITY CLASSIFICATION OF ABSTRACT	20. LIMITATION OF ABSTRACT
Unclassified	Unclassified	Unclassified	UL